

Study for visual color improvement for an organic light emitting diode using a dye-circular-polarizer

WEN JENG LAN, HO SHING WU*

Department of Chemical Engineering and Materials Science, Yuan Ze University, Taoyuan, 32003, Taiwan

There are many key vision indexes that can be used to indicate the visual performances of Flat Panel Displays (FPDs), such as visual sensitivity, contrast ratio, color saturation, viewing angle chromatism, pixel solution and brightness. An Organic Light Emitting Diode (OLED) will be reduced the visual performances by ambient light, including visual sensitivity, contrast ratio, color saturation and viewing angle chromatism. The present study investigated the visual color performances of an organic light emitting diode which is based on the thin-film reflective simulation and commission international de l'Eclairage (CIE) photopic luminous efficiency curve (visual factor) to choose the adaptive optical film. After the simulation and calculation, the presented application uses a mature and convenient method to examine the image color improvement of an OLED that uses a dye-circular-polarizer on the panel. The results clearly showed the excellent performance in improving visual sensitivity by 79.1% in the visual sensitivity region of human eyes (400~700nm), increasing more 12% color saturation in dark, reinforcing the weaknesses of the red and blue organic fluorescent materials, retarding color-chromatism-decay from 48% to 25.4% in the simulated indoor ambient light (490 cd/m²) and from 69.9% to 45.8% in the simulated outdoor ambient light (1375 cd/m²), improving more 40% and 65% color saturations when tilting at 35° and 70° viewing angle for a simulated indoor ambience (490 cd/m²), and improving 73% and 5% more color saturation when tilting at 35° and 70° viewing angle for a simulated indoor ambience (1375 cd/m²), respectively.

(Received November 23, 2011; accepted January 22, 2014)

Keywords: Organic light emitting diode, Iodide-polarizer, Visual reflective sensitivity, Contrast ratio, Color saturation, View angle

1. Introduction

The new generation flat panel displays have progressed well technically and operated in various applications [1-3]. Field panel displays (FPDs) and organic light-emitting diodes (OLEDs) have many characteristic elements (e.g. wide viewing angle, high contrast ratio, high color saturation and rapid response time). OLEDs are recognized to be the greatest potential at the next generation display devices [4-6] and planar lighting sources [7-9]. OLED research had mainly restricted in the academic world until Tang and Vanslyke of Kodak Chemical in 1987 [10] showed for the first efficient organic light-emitting device in a multilayer configuration with significant performance improvement, and functional performance of multi-layer OLEDs. They have received much attention due to their many advantages. Nowadays, small molecular organic light-emitting diodes (SMOLED) made using thermal deposition processes have been utilized for making commercial display products. The design of the multi-layers is placed between the hole injecting anode and the electron injecting cathode. And they are combined in something like a sandwich, including the hole injection layer (HIL), hole transporting layer (HTL), emitting layer (EML), electron transporting layer (ETL), and electron injection layer (EIL). These multi-layers can be designed by using adaptive dopant, codopant and/or cohost mechanisms [11-13] and made by a thermal deposition process [5,10].

Many methods have been employed to upgrade the optical performance of OLEDs. For example, a pyramidal

array light-enhancing layer (pyramidal ALEL) on an organic light-emitting diode panel was optimized to enhance the luminance efficiency experimentally [14]. The emission of light and external coupling in OLEDs has been investigated and the thickness of the indium tin oxide (ITO) layer has been controlled in order to reduce the energy loss in the high-index layer [15]. Furthermore, the rough or textured surfaces [16-17], mesa structures and lenses [18-19] have been manufactured to suppress the waveguide modes and reduce the reflectance in the recent years. However, increasing high light emission compensate the reflection of ambient lights not enough to improve visual image performances and also lead to eyestrain and a short lifetime of the product. As some solutions promote the color gamut of OLEDs, the high efficient organic phosphorescent materials was used to develop visual color saturation for organic electroluminescent displays [20-22]. Although the organic phosphorescent materials are able to improve the color and efficiency of OLEDs, however, they are more expensive to make and have more complex organic sandwich architectures than organic fluorescent materials. Another solutions for improving the color saturation of OLEDs, the color conversion method (CCM) and color filter (CF) was simultaneously used to progress the color saturation of a passive matrix OLED (PMOLED) [23,24], and the masked color filter (MCF) also was promoted to enhance the color performance [25], however, these technologies were complex for making an OLED. On the other hand, the iodide polarizer was proposed to retard color chromatism decay in the ambient lights [26], and another similar

method was used to simulate and investigate the improvement of the color saturation in PMOLED by using a dye polarizer [27,28]. To promote contrast ratio, the optical interference effect was used to develop multi-layer black electrodes by using vacuum deposition technology [29-34]. High contrast solutions, making black matrixes or reducing resistance matrixes of the pixels will reduce visual reflective sensitivity by lithography process technology [35,36]. However, the black electrodes and/or black matrixes are not parts of the original OLED design. They will lead to extra fabrication complexity and costs.

In this study, we use a thin-film optical reflective simulation to investigate the reflection simulation of the panel of the experimental OLED. According to the simulative calculation and commission international de l'Eclairage (CIE) photopic luminous efficiency curve (visual factor), we choose an adaptive dye-circular-polarizer composed of a linear polarizer and a quarter-wavelength phase retarder to improve the visual color performance of the experimental OLED. The theoretical simulation and experimental data are expected to provide information of both great academic and practical significance.

2. Experimental section

2.1. Experimental OLED manufacturing

The experimental OLED was fabricated as the panel of the bottom emission of a passive-matrix OLED (PMOLED). The process flow of the panel of the experimental OLED was followed by Lan and Wu in 2011 [26], which 0.7 mm thickness of a mother glass substrate with an indium tin oxide (ITO) film deposited on the surface of the mother glass with a 150 nm thickness. The average electro-optical property of the experimental ITO substrate provides larger than 85% transmittance in the visible region and less than $10 \Omega/\square$ sheet resistances.

In the process flow of the panel of the experimental OLED, the first step of the process flow included the patterns of the four layers in the thin film, lithography and the etching processes of the ITO substrate. The ITO substrates were purchased from Geomatec (Yokohama/Japan). About the procedures of the first step, it included the metal alloy pattern of the external conductive line (e.g. silver), the pattern of the transparent electrode (e.g. indium tin oxide), the insulator pattern of the pixel definition (e.g. polyimide) and the separator pattern of the cathode metal (e.g. negative-photoresist). In the second step, an evaporator was used to make the multi-organic layers by side-by-side process and cathode metal (e.g. aluminum) layer [5,10]. The material of hole injection layer (HIL) which reduces the energy barrier in between ITO and hole transport layer (HTL) is therefore beneficial to enhance charge injection at the interfaces and ultimately improve power efficiency of the device, the materials of HIL are that starburst amorphous materials, 4, 4', 4''-tris(3-methyl-phenyl-phenylamino)triphenylamine (m-MTDATA) can be doped by 3% strong molecular

acceptors tetrafluoro - tetracyano - quinodimethane (F₄-TCNQ) in the controlled co-evaporation [32]. The material of HTL has a "bi-phenyl" center core which is N,N'-bis(1-naphthyl)-N,N'-diphenyl-1,1'-biphenyl-4,4'-diamine (NPB). The materials of emitting layer (EML) utilize the fluorescent dopants in the guest-host doped emitter system, the red emitting materials that are 2% 4-(dicyanomethylene)-2-tert-butyl-6(1,1,7,7-tetramethyljulolidin-4-yl-vinyl)-4H-pyran (DCJTb) to be doped in the molar ratio (3/2) of 5,6,11,12-tetraphenyl-naphthacene (Rubrene) to tris(8-hydroxyquinolino)aluminum (Alq₃) of a cohost system, the green emitting materials that are 6% GD-206 of Idemitsu Kosan to be doped in BH-120 of Idemitsu Kosan, and the blue emitting materials that are 2% BD-52 of Idemitsu Kosan to be doped in BH-120 of Idemitsu Kosan. The material of electron transport layer (ETL) is a tris(8-hydroxyquinolino)aluminum (Alq₃). The material of electron injection layer (EIL) is a lithium fluoride (LiF), an effective cathode Al for OLEDs could be constructed by interposing a thin LiF layer between Al and Alq₃ [38,39]. These organic materials were purchased from Syntec GmbH (Wolfen/Germany), Aldrich (Missouri/MO), Eastman Kodak (Rochester/NY) and Idemitsu Kosan (Mojji/Japan), respectively. In consideration of getting a high production yield, the thicker thicknesses of organic material layers and cathode metal-Al layers were considered to avoid the defect issues caused by the spike of ITO, pin holes of films, thermal stability of light-emitting and particles [40-42]. The thicknesses of HIL/HTL/EML(R/G/B)/ETL/EIL and cathode metal-Al were 200/20/(R:20/G:18/B:25)/20/0.1 and 300 nm, respectively. After the second step, this glass substrate was encapsulated by an encapsulation glass substrate with getter to control the H₂O/oxygen-free environment. Finally, the encapsulated substrate was scribed, broken according to the size of the design and assembled with the driver IC which is able to tune gamma curves in relation to grayscale and brightness in this step [43].

The experimental PMOLED panel was formatted in the specification of 1.5"-128RGBx128 with 262,144 colors, which has color saturation compared with the standard of the National Television System Committee (NTSC) to be 59.4%, its red coordinates (x, y) of CIE₁₉₃₁ are (0.630, 0.354), the green coordinates (x, y) of CIE₁₉₃₁ are (0.294, 0.630) and the blue coordinates (x, y) of CIE₁₉₃₁ are (0.145, 0.193) and the synthetic white luminance is 145 (cd/m²) when turning on red, green and blue simultaneously.

2.2. The property of the dye-circular-polarizer

The optical films are deposited and laminated on the surface of a substrate to change the conveyors of wavelength, including the polarizer, phase compensator, brightness enhancement film, light collimated sheet, diffusion film, reflector, anti-reflection film and anti-glare film. A polarizer is a device that converts a beam of electromagnetic waves (light) of undefined or mixed polarization into a beam with well-defined polarization.

The polarizer is an important component in liquid crystal display (LCD) fields. It can polarize the light from the backlight source of the LCD. Conversion of a wave from linear to circular polarization may be effected by either transmission or reflection. In a free space at millimeter wavelengths, reflection circular polarizers are preferable to their less compact transmission counterparts [44]. The applied dye-circular-polarizer is the combination of a linear polarizer and a quarter-wavelength phase retarder. A strong ambient light passes through the linear polarizer layer, thus turning into horizontal oriented light. As this light is reflected off the surface of an OLED, it is now spinning in the opposite direction. This reverse spinning light reflected off the surface of the OLED is 90 degree different from the transmission axis of only a linear polarizer. Because of its orientation, the linear polarizer absorbs the reflected light to cancel it out so that it is not observed by the view [45,46]. Another function of polarizers is that they are able to protect the panel from scraping. Previous studies have discussed the optical properties of dye polarizers [47,48] and a new model has been developed to account for the dependence of optical anisotropy [49]. About the relative compositions of a dichroic dye in the applied dye-polarizer, they are like some polymer formulas with azo, polycyclic, or anthraquinone compounds (or mixtures) [50-53].

In general, dye-circular-polarizers have better transparency in the red and blue regions of visible light that are able to enhance the color saturation of an OLED and better temperature tolerance. That is better for portable applications in the outdoors than typical iodine-circular-polarizer. [45,50]. Hence, a common dye-circular-polarizer with a convenient are laminated panel display is considered this study.

2.3. Measurement inspection

After the fabrication, the electro-optical performance of the panel of the experimental PMOLED was verified and confirmed by the following instruments and measurement inspections. The color performances in index of the CIE₁₉₃₁, color gamut (color saturation) and the current-luminance-voltage (ILV) curve of the OLED are necessary to verify. Color saturation and the current-luminance-voltage (ILV) curve of the experimental PMOLED were measured by a Minolta Chroma Meter CS-1000 (USA). Different light conditions of indoor ambience and outdoor ambience were simulated using the DMS-505 type of the autronic-MELCHERS GmbH (German). The transparent performance of the dye-polarizer and the reflecting performance in the panel of the OLED were measured by using a Hitachi U4100 system (Japan).

3. Results and discussion

3.1. Effects of the visual sensitivity of human eyes

The multi-layer thin-films of OLEDs are deposited on the substrate, including the transparent anode, the organic multi-layers and the metal cathode. The reflectance of the panel of an OLED can be described by the theory of thin-film simulation which has a like transfer matrix of thin-film optical filters [26-28,54]. There are fundamentally difficult ratiocinations and definitions associated with the expression of reflectance (R)

$$\delta = 2\pi N / d \quad (1)$$

$$R(\lambda) = [(y_0 - y_1)/(y_0 + y_1)][(y_0 - y_1)/(y_0 + y_1)]^* \quad (2)$$

where N is often complex refractive index, d is the wave allows for a shift in the z coordinate of the medium from 0 to d , y_0 and y_1 are phase indices that are the admittance of the incident medium and the admittance of the substrate upon which the thin-film system is deposited, and the asterisk donates the complex term. A high contrast OLED can also be fabricated by the theory of the method reported by previous work [27]. The concept is based upon using these materials with the gradient or graded refractive index to development a high contrast OLED [55].

The visual sensitivity of human eyes is non-linear and changes according to the wavelength. Thin-film simulation and the CIE photonic luminous function (visual factor) are shown in Fig. 1. Fig. 1 shows that the reflective simulation of the panel of the experimental OLED which has a high amount of green reflective wavelength region (525nm ~ 580nm) for the visual sensitivity of human eyes. In this study, the proposed technique is a mature and convenient method to improve the image color improvement of an OLED that uses a functional optical film. There were the transmittances of some optical films, as shown in Fig. 2. In similarity, it displayed a dye-circular-polarizer with better transparency in the red and blue region and lower transparency in the green region in the visible light range, which was ratiocinated to improve the visual sensitivity of human eyes. According to the results of Figs. 1 and 2, we could apply the optical transmittance property of a dye-circular-polarizer to reduce the effect of reflective light on human eyes that is caused by ambient light. According to the result of Lan and Wu in 2011 and 2012 [26,28], the visual sensitivity of human eyes was improved when utilizing an iodine-circular-polarizer or a dye-circular-polarizer on the panel of the OLED, as shown in Fig. 3. Using an iodine-circular-polarizer or a dye-circular-polarizer on the panel of OLED can obviously reduce the visual reflective sensitivity by 91.2% or 86.6% in the visual sensitivity region of human eyes on the panel of the OLED, respectively. Other optical films, such as AR (anti-reflection film) and AG (anti-glare film) on the panel of OLED didn't reduce the visual reflective sensitivity.

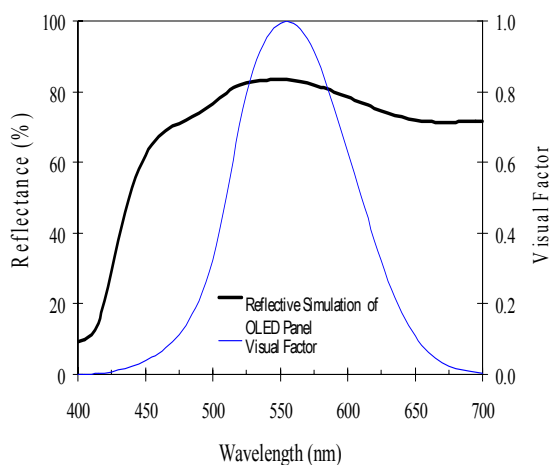


Fig. 1. The simulation of the reflectance of the experimental OLED and CIE photonic luminous (visual factor).

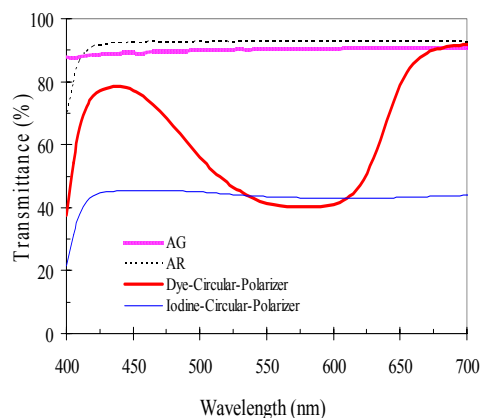


Fig. 2. Transmittances of an antiglare film (AG), an antireflective film (AR), a dye-circular-polarizer and an iodine - circular - polarizer. These transmittances are measured by Hitachi U4100 system.

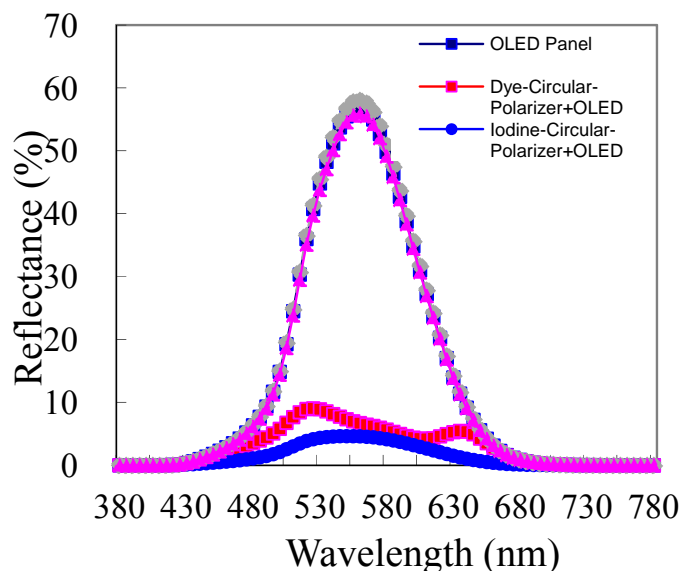


Fig. 3. The reflectance of the OLED with different optical films (antiglare film (AG), antireflective film (AR), dye-circular-polarizer and iodine-circular-polarizer) for visual reflective sensitivity of human eyes [26,28].

3.2 Effects of CIE₁₉₃₁ and color saturation in dark room

According to rules of color performance defined by CIE₁₉₃₁, the red, green and blue coordinates (x,y) of CIE₁₉₃₁ and color saturation are comparable with the standards of the National Television System Committee (NTSC). Larger gamuts offer clearer discrimination for the vision of human eyes. The color saturation is a key point of displays [56]. We measured the CIE₁₉₃₁ index and color saturation of the experimental OLED by a Minolta Chroma Meter CS-1000, as listed in Table 1 [26-28]. According to the result in Table 1, an iodine-circular-polarizer on the panel of OLED doesn't

obviously improve color saturation in the panel of the OLED. The proposed technique is using a dye-circular-polarizer on the panel of OLED to improve color saturation in the panel of the OLED, that achieved better color performance and increased more 12% color saturation. The CIE₁₉₃₁ index and color saturation of the experimental OLED with a dye-circular-polarizer and light blue (e.g., 3% BD-102 of Idemitsu Kosan doped in BH-120 of Idemitsu Kosan) and orange (e.g., 2.5% p1 of Idemitsu Kosan doped in BH-120 of Idemitsu Kosan) were studied. Organic fluorescent materials was instead of blue (e.g., 2% BD-52 of Idemitsu Kosan to be doped in BH-120 of Idemitsu Kosan) and red (e.g., 2% DCJTb doped in the ratio of three Rubrene to two Alq₃ of a cohost system)

fluorescent materials. According to the information provided by organic fluorescent materials [5,22,57-59], the lifetime and efficiency of blue and red organic fluorescent materials are weaker than those of light blue and orange ones. The purpose of the combination of a dye-circular-polarizer and light blue and orange organic fluorescent materials is the improvement of device

characteristics such as lifetime, efficiency and color saturation [28]. Although the organic phosphorescent materials are able to improve the lifetime and efficiency of blue and red devices of OLEDs, however, they are more expensive to make and more complex organic sandwich architectures than organic fluorescent materials [21,22].

Table 1. Color saturation of the experimental OLED [26-28].

CIE ₁₉₃₁	OLED with Blue and Red organic fluorescent materials			OLED with Light Blue and Orange organic fluorescent materials	
	Without Polarizer	With		Without	With
		Iodine-Polarizer	Dye-Polarizer	Dye-Polarizer	Dye-Polarizer
Red	x	0.630	0.632	0.642	0.626
	y	0.354	0.354	0.338	0.364
Green	x	0.294	0.295	0.278	0.311
	y	0.630	0.630	0.622	0.633
Blue	x	0.145	0.145	0.139	0.151
	y	0.193	0.197	0.152	0.250
NTSC, %		59.4	59.1	66.5	51.7
					59.7

3.3 Effects of contrast ratio and color saturation in the different ambient lights

According to the visual sensitivity of human eyes in ambient light, we also attempted to conduct a discussion of the contrast ratio (CR) of a display in this ambience. The contrast ratio indicates the amount of difference that can be used to discriminate between a pixel that is fully on and one that is off in the reflection of ambient light. The contrast ratio is presented in Eq. (3) [34,60,61].

$$CR=(L_{on}+R \times L_{amb}) / (L_{off}+R \times L_{amb}): \quad (3)$$

in which CR, L_{on} , L_{off} and L_{amb} are contrast ratios, the luminance of the OLED when turned on, the luminance of the OLED when turned off and the luminance of ambient light, respectively.

It was very effective for interrupting the ambient reflective light by the performance of circular-polarizer, which was studied for improving the image contrast ratio performance of an OLED by Lan and Wu [26,28]. According to the simulated ambient lights by Lan and Wu [27], the luminance of indoor ambient light (490 cd/m²) and outdoor ambient light (1375 cd/m²) are simulated by means of the DMS-505 system of the autronic MELCHERS GmbH. A brightness value was obtained when utilizing a dye-circular-polarizer on the panel of an OLED in different simulated ambient light. The dye-circular-polarizer is able to increase the contrast ratio of the panel by 2.4 and 2.7 times in simulated indoor ambience and outdoor ambience, respectively [27,28].

In the dark ambience, the spectral stimulus on the panel of the experimental OLED with optical polarizer was modified by Lan and Wu [27]. The ratiocination

equation of color saturation in ambient light was re-modified. Due to the 2nd reflective factor being small, we can neglect it. Here were the modified equations, by our previous study[27].

$$X = \int_{400}^{700} (Q_{\lambda} \bar{x}(\lambda) \times T_{Dye-Polarizer}(\lambda) + L(\lambda) \times R_{Dye-Polarizer}(\lambda)) d\lambda \quad (4)$$

$$Y = \int_{400}^{700} (Q_{\lambda} \bar{y}(\lambda) \times T_{Dye-Polarizer}(\lambda) + L(\lambda) \times R_{Dye-Polarizer}(\lambda)) d\lambda \quad (5)$$

$$Z = \int_{400}^{700} (Q_{\lambda} \bar{z}(\lambda) \times T_{Dye-Polarizer}(\lambda) + L(\lambda) \times R_{Dye-Polarizer}(\lambda)) d\lambda \quad (6)$$

in which, Q_{λ} , $\bar{x}(\lambda)$, $\bar{y}(\lambda)$ and $\bar{z}(\lambda)$, $L(\lambda)$ and $R_{Dye-Polarizer}(\lambda)$ are given stimulus, color-matching functions, the strength of ambient light and the reflectance of the dye-circular-polarizer composed of a linear polarizer and a quarter-wavelength phase retarder, respectively. Associated x and y values are chromaticity coordinates, which may be computed from Eqs. 4 to 6.

$$x = \frac{X}{X + Y + Z} \quad (7)$$

$$y = \frac{Y}{X + Y + Z} \quad (8)$$

The simulation and instrumental measurement of the color saturation of the panel of the experimental OLED are listed in Table 2. The result shows similar values in the simulation and instrumental measurement of the color

saturation of the panel of the experimental OLED. And the proposed technique was able to achieve better color performance, increasing more 12%, 43% and 78% color

saturation in a dark ambience, an indoor ambience (490 cd/m²) and an outdoor ambience (1375 cd/m²), respectively.

Table 2. Effect of color saturation with a dye-circular-polarizer on the panel of OLED or not [27].

Simulating Ambiance	Instrument		Simulation
	Without Dye-Circular-Polarizer	With Dye-Circular-Polarizer	
Dark	59.4 %	66.5 %	65.7 %
Indoor (490 cd/m ²)	30.9 %	44.3 %	50.4 %
Outdoor (1375 cd/m ²)	17.9 %	32.2 %	33.9 %

For the laminated dye-circular-polarizer on the panel of the OLED and tilting at the larger angles (at 0°, 35° and 70°) in the simulated indoor ambience (490 cd/m²), the color saturations of the OLEDs are shown in Figs. 4(a) and (b). They clearly show more 43%, 40% and 65% color saturations with a dye-circular-polarizer on the panel of the OLED. Similarly, for the laminated dye-circular-polarizer on the panel of the OLED and tilting at 0°, 35° and 70° in the simulated outdoor ambience (1375 cd/m²), the color saturations of the OLEDs are shown in Figs. 4(c) and 4(d). They can also clearly achieve 80%, 73% and 5% more color saturations with a dye-circular-polarizer on the panel of the OLED, respectively.

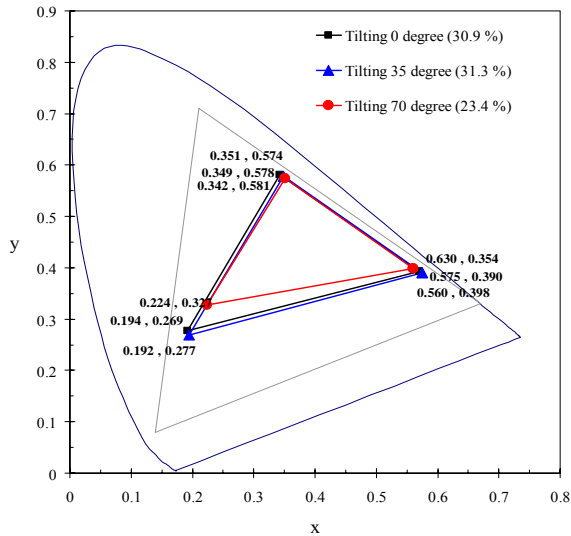


Fig. 4a. The CIE₁₉₃₁ Chromaticity Diagram displays the CIE₁₉₃₁ index and color saturation of the OLED without a dye-circular-polarizer in a simulated indoor ambience (490 cd/m²).

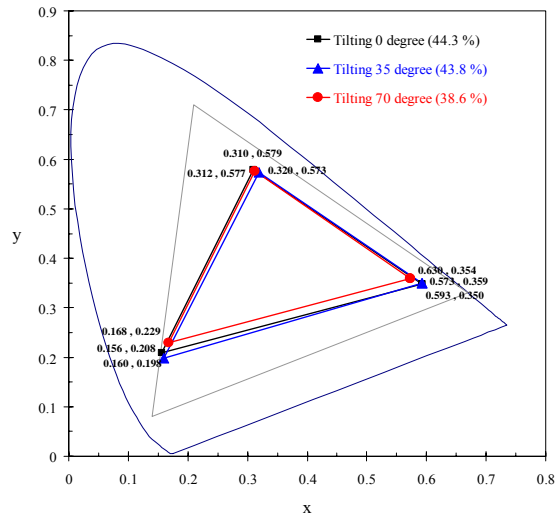


Fig. 4b. The CIE₁₉₃₁ Chromaticity Diagram displays the CIE₁₉₃₁ index and color saturation of the OLED with a dye-circular-polarizer in a simulated indoor ambience (490 cd/m²).

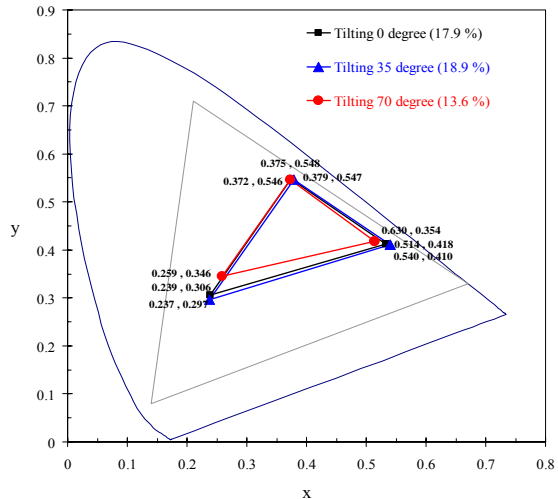


Fig. 4c. The CIE₁₉₃₁ Chromaticity Diagram displays the CIE₁₉₃₁ index and color saturation of OLED without a dye-circular-polarizer in a simulated outdoor ambience (1375 cd/m²).

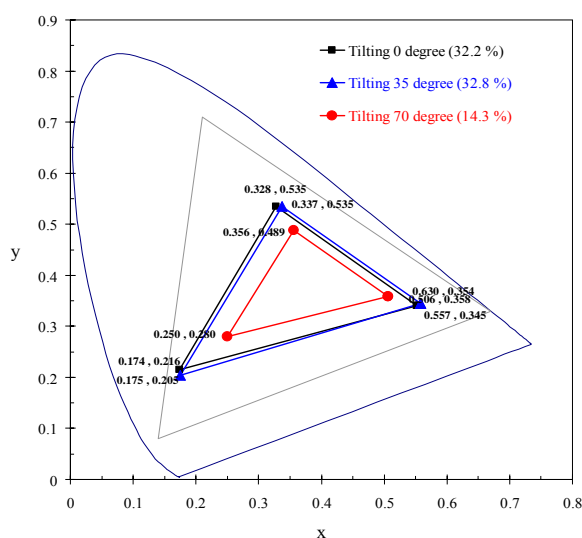


Fig. 4d. The CIE₁₉₃₁ Chromaticity Diagram displays the CIE₁₉₃₁ index and color saturation of the OLED with a dye-circular-polarizer in a simulated outdoor ambience (1375 cd/m²).

Image performances can be resolved into many characteristic elements, such as pixel solution, brightness, viewing angle, response time, visual reflective sensitivity, contrast ratio and color saturation. Light reflectance is expressed as a percentage and states how much of the light falling on a surface is reflected back. Generally, the reflect light of surface of a display will be caused by a strong ambient light. It will reduce the readability of human eyes and cause a decrease in the visible contrast ratio, color saturation of the screen image for the visual sensitivity of human eyes. The lamination function of the dye-circular-polarizer is easy to use and well developed for the production of displays. In the application of OLEDs, it clearly improves the visual sensitivity of human eyes, the visual contrast ratio and color saturation of the display in the ambient lights, and protects the panel's surface from scraping.

4. Conclusion

In this study, the panel of an OLED has been successfully ratiocinated with the application of basic thin-film simulation. According to the results of thin-film reflective simulation and visual factor, the proposed technique applied a dye-circular-polarizer composed of a linear polarizer and a quarter-wavelength phase retarder on the panel of an OLED. This method was able to reduce the reflected light for visual reflective sensitivity of the human eye by 86.6% in ambient light, and improve the color performance to 12%, 43% and 78% times in a dark, an indoor (or office) ambience and an outdoor ambience, respectively. In a practical application, due to the weaknesses related to lifetime and the efficiency of red and blue organic fluorescent materials, this study used

light blue and orange organic fluorescent materials. It was also able to improve 40% and 65% more color performance when tilting at 35° and 70° viewing angle for a simulated indoor ambience and improved 73% and 5% more color performance when tilting at 35° and 70° viewing angle for a simulated indoor ambience, respectively.

References

- [1] J. Kalinowski, Organic Light-Emitting Diodes: Principle, Characteristics and Processes. New York: Marcel Dekker, (2005)
- [2] J. H. Lee, D. N. Liu, S. T. Wu, Introduction to Flat panel Displays, John Wiley & Sons Ltd, Chichester, England (2008).
- [3] A. K. Bhowmik, B., Z. Li, P. J. Bos, Mobile Displays, John Wiley & Sons Ltd, Chichester, England (2008).
- [4] B. Geffroy, P. le Roy, C. Prat, Polymer International, **55**, 572 (2006).
- [5] C. H. Chen, S. W. Huang, OLED: Materials and Device of Dream Displays, Wunan, Taipei, Taiwan (2007).
- [6] Z. Li, M. Hong, Organic light-emitting materials and devices, John Wiley & Sons Ltd, Chichester, England (2008).
- [7] J. Kido, K. Hongawa, K. Okuyama, K. Nagai, Appl. Phys. Lett., **64**, 815 (1994).
- [8] S. Reineke, F. Lindnerl, G. Schwartzl, N. Seiderl, K. Walzerl, B. Lusem, K. Leo, Nature, **459**, 234 (2009).
- [9] C. H. Chen, White OLED for Lighting, Wunan, Taipei, Taiwan (2009).
- [10] C. W. Tang, S. A. VanSlyke, Appl. Phys. Lett., **51**, 913 (1987).
- [11] C. W. Tang, S. A. VanSlyke, C. H. Chen, J. Appl. Phys., **65**, 3610 (1989).
- [12] R. H. Young, C. W. Tang, A. P. Marchetti, Appl. Phys. Lett., **80**, 874 (2002).
- [13] T. H. Liu, C. Y. Iou, C. H. Chen, Appl. Phys. Lett., **83**, 5241 (2003).
- [14] M. L. Chen, A. C. Wei, H. P. Shieh, Jpn. J. Appl. Phys., **46** (4A), 1521 (2007).
- [15] M. H. Lu, J. C. Sturm, J. Appl. Phys., **91**, 595 (2002).
- [16] A. A. Bergh, R. H. Saul, U.S. Patent **3**, 739, 217 (1973).
- [17] I. Schnitzer, E. Yablonovitch, C. Caneau, T. J. Gmitter, A. Scherer, Appl. Phys. Lett., **63**, 2174 (1993).
- [18] S. Möller, S. R. Forrest, J. Appl. Phys., **91**, 3324 (2002).
- [19] M. K. Wei, I. L. Su, Optics Express **12**, 5777 (2004).
- [20] M. A. Baldo, D. F. O'Brien, Y. You, A. Shoustikov, S. Sibley, M. E. Thompson, S. R. Forrest, Nature, **395**, 151 (1998).
- [21] M. A. Baldo, M. A., S. Lamansky, P. E. Burrows, M. E. Thompson, S. R. Forrest, Appl. Phys. Lett., **75**, 4 (1999).
- [22] A. Kohler, J. S. Wilson, R. H. Friend, Adv. Mat., **14**, 701 (2002).
- [23] K. Sakurai, H. Kimura, K. Kobayashi, T. Suzuki,

- Y. Kawamura H. Saito, M. Nakatani Niigata, Processings of IDW, 1269 (2004).
- [24] Y. Terao, M. Kobayashi, N. Kanai, R. Makino, C. Li, Y. Kawamura, K. Kawaguchi, T. Saito, H. Hashida H. Kimura, Shanghai, Optical Fiber Communication and Optoelectronics Conference, 245 (2007).
- [25] C. Y. Feng, T. C. Chen, W. J. Lan, C. C. Chiang, Taiwan Patent I296181 (2008).
- [26] W. J. Lan, H. S. Wu, J. Optoelectron. Adv. Mater., **13**, 490 (2011).
- [27] W. J. Lan, H. S. Wu, AICHE J., **58**(6) 1755 (2012).
- [28] W. J. Lan, H. S. Wu, Can. J. Chem. Eng., **90**, 1246 (2012).
- [29] L. S. Hung, J. K. Madathil, US Patent **6**, 429, 451 B1 (2002).
- [30] P. Y. Chen, M. Yokoyama, H. Y. Ueng, Jpn. J. Appl. Phys. **49**, 12102 (2010).
- [31] Z. H. Huang, W. M. Su, X. T. Zeng, SIMTech Technol. Rep., **8**, 4 (2007).
- [32] O. H. Kim, T. J. Ahn, US Patent 7, 071, 613 B2 (2006).
- [33] S. H. Hwang, M. K. Seo, J. H. Kang, J. Y. Yang, S. Y. Kang, J. Kor. Phys. Soc., **55**, 2 (2009).
- [34] P. G. Hofstra, A. N. Krason, US Patent 6, 411, 019 B1 (2002).
- [35] B. D. Lee, Y. H. Cho, M. H. Oh, S. Y. Lee, Mater. Chem. Phys. **112**, 734 (2008).
- [36] W. J. Lan, C. C. Chang Chien, Taiwan Patent I228, 382 (2005).
- [37] J. Drechsel, M. Pfeiffer, X. Zhou, A. Nollau, K. Leo, Synthetic Metals, **127**, 201 (2002)
- [38] L. S. Hung, C. W. Tang, M. G. Mason, Appl. Phys. Lett., **70**, 152 (1997).
- [39] G. E. Jabbour, V. Kawabe, S. E. Shaheen, J. F. Wang, M. M. Morrell, B. Kippelen, N. Peyghambarian, Appl. Phys. Lett., **71**, 1762 (1997).
- [40] N. M. Dos Anjos, H. Aziz, N. X. Hu, Z. D. Popovic, Organic Electronics, **3**, 9 (2002).
- [41] M. Fujihira, L. M. Do, A. Koike, E. M. Han, Apply Phys. Lett., **68**, 1787 (1996).
- [42] J. McElvain, H. Antoniadis, M. R. Hueschen, J. N. Miller, D. M. Roitman, J. R. Sheats, R. L. Moon, J. Appl. Phys., **80**, 6002 (2002).
- [43] A. Sempel, M. Buchel, Organic Electronics, **3**, 89 (2002).
- [44] E. V. Jull, Electron. Lett., **15**, 423-424 (1979).
- [45] Y. C. Cheng, H. C. Lin, Taiwan Patent 594,067 (2004).
- [46] OptiGrafix™, <http://www.optigrafix.com/circular.htm>
- [47] Y. Dirix, T. A. Tervoort, C. Bastiaansen, Macromolecules, **28**, 486 (1995).
- [48] Y. Dirix, T. A. Tervoort, C. Bastiaansen, Macromolecules, **30**, 2175 (1997).
- [49] S. E. Han, I. S. Hwang, J. Polym. Sci., **40**, 1363 (2002).
- [50] Y. Matsuzaki, R. Oil, R. Imai, K. Takuma, H. Itoh, US Patent 5, 698, 682 (1997).
- [51] I. Khan, G. Y. A. Bobrov, L. Y. Ignatov, E. Y. Shishkina, P. I. Lazarev, A. V. Kurbatov, US Patent 6, 049, 428 (2000).
- [52] S. H. Liu, Y. C. Lin, W. S. Tzeng, J. H. Ma, K. L. Cheng, L. L. Lai, US Patent 6, 861, 106 B2 (2005).
- [53] C. Y. Hung, Dichroic Dye Application in Polyvinyl Alcohol Polymerizing Films, Taiwan NTUT, Master Thesis (2008).
- [54] H. A. Macleod, Thin-film Optical Filters, Institute of Physics Pub., Philadelphia (2001).
- [55] F. Zhu, O. K. Soo, T. L. Wei, H. Xiaotao, LEOS, The 18th Annual Meeting of the IEEE, 589 (2005).
- [56] J. A. Castellano, Handbook of Display Technology, Academic Press Inc., New York (1992).
- [57] S. Chew, P. Wang, Z. Hong, S. Tao, J. Tang, C. S. Lee, N. B. Wong, H. Kwong, S. T. Lee, Appl. Phys. Lett., **88**, 183504 (2006).
- [58] Q. Huang, K. Walzer, M. P. Feiffer, V. Lyssenko, G. He, K. Leo, Appl. Phys. Lett., **88**, 113515 (2006).
- [59] J. H. Lee, Y. H. Ho, T. C. Lin, C. F. Wu, J. Electro. Soc., **154**, J226 (2007).
- [60] W. F. Xie, Y. Zhao, C. N. Li, S. Y. Liu, Opt. Exp., **14**, 2006; 7954 (2006).
- [61] W. F. Xie, H. Y. Sun, C. W. Law, C. S. Lee, S. T. Lee, S. Y. Liu, Appl. Phys., A85, (2006).

*Corresponding author: cehsu@saturn.yzu.edu.tw